Asociación Argentina
de Mecánica Computacional

Mecánica Computacional Vol XXV, pp. 3-20
Alberto Cardona, Norberto Nigro, Victorio Sonzogni, Mario Storti. (Eds.)
Santa Fe, Argentina, Noviembre 2006

# NUMERICAL PREDICTIONS OF TRANSIENT AND STEADY RHEOMETRIC FUNCTIONS OF POLYETHYLENE MELTS THROUGH A SPECTRAL TENSORIAL CONSTITUTIVE EQUATION

**Marta B. Peirotti, Mariel L. Ottone and Julio A. Deiber**

*Instituto de Desarrollo Tecnológico para la Industria Química*
*INTEC (UNL - CONICET)*
*Güemes 3450, S3000GLN-Santa Fe, Argentina, treoflu@ceride.gov.ar*

**Keywords**: Polymer Melt Viscoelasticity, Phan-Thien and Tanner Model, Relaxation Time Spectrum, Transient Rheometric Functions

**Abstract:**
At present, one can find in the literature a high number of constitutive equations in order to quantify, with varying precision, the stress tensor of viscoelastic materials through rheometric measurements. These equations may be basically classified as integral and differential models. Also, these models may be expressed through the addition of several stress modes by using a spectrum of relaxation times, which is obtained from linear viscoelastic properties of materials, tested in the mechanical spectrometer. Therefore, the choice of a tensorial constitutive equation to predict computationally complex flow kinematics in the processing operations of materials is a rather difficult task with this wide menu. This undesired situation occurs mainly when one needs a rather complete set of rheometric functions characterizing the material under consideration. In this work we explore the capability of the spectral Phan-Thien and Tanner model to characterize transient and steady shear and elongational rheometric functions of linear and branched, and low and high density polyethylene melts, involving different microstructures. For these specific purposes, precise numerical programs are carried out to consider different mechanical histories involving experimental data already reported in the literature. A discussion concerning the prediction quality of the rheological model proposed is presented and some physical aspects involving requirements for further research are provided.

## 1 INTRODUCTION

A high number of integral and differential constitutive equations are available in the rheological literature in order to quantify, with varying precision, the stress tensor of viscoelastic materials, once the involved rheological parameters have been evaluated through rheometric measurements. Nevertheless, the selection of an appropriate constitutive equation for a material under study (for instance, a polymer melt of the processing industry) is not a simple task having into account that in practice one usually finds several difficulties; the most relevant in this sense are: (a) the number of experimental data available concerning different rheometric tests are not enough to characterize the required rheological parameters without ambiguity, (b) the constitutive equation selected is not able to fit simultaneously steady and / or transient experimental data of both shear and elongational rheometric functions with the same set of rheological parameters. Difficulty (a) is the most frequently found, both in basic research works and in industrial laboratories. This situation is a consequence of that the full rheometric characterization of a given material may result a very expensive and time-consuming job. The unavailability of commercial rheometers allowing true elongational tests (mainly for fluids and melts) is an additional disadvantage. Thus under these circumstances a few rheometric data are used to select a constitutive equation to be used in design and control of processing operations, where some hypothesis must be introduced, placing questions on the validity of the results thus obtained. Difficulty (b) is however more prone to scientific research when enough experimental data are available. Here it is relevant the consideration of a spectrum of relaxation times to fulfill a crosscheck when different mechanical histories are considered. Therefore, one needs to have available robust algorithms to test constitutive equations with these data, and to end up with the most appropriate one for further calculations.

Based on this brief discussion, in this work we explore the capability of the spectral Phan-Thien and Tanner (PTT) model to characterize transient and steady shear and elongational rheometric functions of linear and branched, and low and high-density polyethylene melts, involving different microstructures. For these specific purposes, precise numerical programs are carried out to consider different mechanical histories involving experimental data already reported in the literature. A discussion concerning the prediction quality of the PTT model is presented, and some physical aspects placing requirements for further research are provided. Thus we carried out a rheometric study of the spectral PTT model in order to evaluate rheological parameters of the branched low density polyethylene melt (LDPE9) and the linear low (LLDPE1) and high density (HDPE1) polyethylene melts, with experimental data reported by Bernnat (2001) (the codes used for samples in that work are kept here) involving both the shear rate and elongational viscosities, and the linear viscoelastic rheometric functions like the storage and loss modules. In this work, all rheological calculations are carried out with experimental data from master curves at 190 $^{o}$C. They were measured in a Rheometrics DSR 200 (Bernnat, 2001).

## 2 RHEOLOGICAL MODEL

The spectral PTT model with *M*-modes of effective relaxation times is based on the microstructure stress tensor expressed $\underline{\underline{\tau}}_{p} = \sum_{m=1}^{M} \underline{\underline{\tau}}_{m}$, which is a part of the total extra stress tensor $\underline{\underline{\tau}} = \underline{\underline{\tau}}_{p} + \underline{\underline{\tau}}_{s}$, where $\underline{\underline{\tau}}_{s} = 2\eta_s \underline{\underline{D}}$ is associated with retardation effects involving viscosity $\eta_s$ and the rate of deformation tensor $\underline{\underline{D}}$. In this sense, one expresses,

$$\underline{\underline{\tau}}_m + \lambda_m^e \frac{\delta}{\delta t} \underline{\underline{\tau}}_m = 2\lambda_m^e g_m \underline{\underline{D}} \quad , \qquad m = 1...M \tag{1}$$

Each one of these equations involves an effective relaxation time $\lambda_m^e$, which depends on the stress field as indicated below (Eq. (3)). The time derivative on the right side of Eq. (1) is expressed,

$$\frac{\delta}{\delta t} \underline{\underline{\tau}}_m = \frac{D}{Dt} \underline{\underline{\tau}}_m - \underline{\underline{L}} \cdot \underline{\underline{\tau}}_m - \underline{\underline{\tau}}_m \cdot \underline{\underline{L}}^T \quad , \qquad m = 1...M \tag{2}$$

which is designated the Gordon-Schowalter non-affine time-convective derivative, (see Gordon and Schowalter, 1972). Here $\underline{\underline{L}} = \underline{\nabla} \cdot \underline{v} - \chi \underline{\underline{D}}$ is the effective velocity gradient tensor. Also $\eta_s = \eta_p (1-\alpha)/\alpha$ and $\eta_p = \sum_{m=1}^{M} \lambda_m g_m$ ; consequently the instantaneous elastic response of the PTT model is obtained for $\alpha = 1$. Consistently the zero shear rate viscosity of the melt is expressed $\eta_o = \eta_p + \eta_s$.

In the PTT model, each mode of effective relaxation time is a function of the stress tensor, and it may be expressed,

$$\lambda_m^e = \lambda_m / K_m = \lambda_m / exp\left[ \frac{\xi}{g_m} tr \underline{\underline{\tau}}_m \right] \tag{3}$$

The spectrum of relaxation times $\{\lambda_m, g_m\}$ of the PPT model for each polymer melt is determined first through linear viscoelastic experimental data available in the literature (Bernnat, 2001). Then other rheological parameters like $\alpha$, $\chi$ and $\xi$ are determined through experimental data concerning the shear and elongational viscosities functions. Finally when the PTT model is fully characterized for each polymer melt, one is able to study the numerical predictions of relevant transient rheometric functions. Once this process is finished, the PTT model may be used in the prediction of more complex flows of the polymer processing industry.

| Polyethylene Samples | $M_w$ [Da] | $M_w / M_n$ | $\eta_o$ [Pa s] | Density [kg/m$^3$] |
|---|---|---|---|---|
| HDPE1 | 205000 | 34 | 275000 | 958 |
| LLDPE1 | 105000 | 3.0 | 12650 | 920 |
| LDPE9 | 115000 | 6.8 | 5740 | 921 |

Table 1. Values of mass average molecular weight $M_w$, polydispersity $M_w / M_n$, zero shear rate viscosity $\eta_o$ and density of the three polyethylene melts under study here, as reported by Bernnat (2001).

Below, sections describe the sequence of steps followed here to characterize polyethylene melt samples LDPE9, LLDPE1 and HDPE1, and also indicate the numerical programs developed to carry out the fitting of experimental data and the predictions of rheometric functions. Some relevant data concerning these polymer melts are reported in Table 1.

## 2 RHEOMETRIC CHARACTERIZATION OF MELTS IN THE LINEAR VISCOELASTIC RESPONSE

The viscoelastic constitutive equation must satisfy rheometric data obtained within the asymptotic behavior of linear viscoelasticity. For this purpose, we use experimental data reported in the literature (Bernnat, 2001), for the storage $G'$ and loss $G''$ modules as functions of frequency $\omega$, at a small constant shear rate. Therefore, these rheometric functions in terms of the spectrum of relaxation times are,

$$G'(\omega)=\sum_{m=1}^{M} g_m \frac{\lambda_m^2\omega^2}{\left(1+\lambda_m^2\omega^2\right)} \tag{4}$$

$$G''(\omega)=\sum_{m=1}^{M} g_m \frac{\lambda_m\omega}{\left(1+\lambda_m^2\omega^2\right)} \tag{5}$$

These modules may be also expressed through the loss component of the dynamic viscosity $\eta'(\omega)=\frac{G''(\omega)}{\omega}$, and its elastic counterpart $\eta''(\omega)=\frac{G'(\omega)}{\omega}$. Thus, one readily obtains the modulus of the complex dynamic viscosity $\eta^*(\omega)=\sqrt{\eta'(\omega)+\eta''(\omega)}$ as a representative value of the shear rate viscosity at the asymptotic limit of small shear rates.

The algorithm used to fit experimental data is composed of two parts. One involves a linear least squares procedure with linear inequality constraints, which impose that $\{\lambda_m, g_m\}$ must be positive values for physical meanings (see, for example, Deiber et al., 1997; Peirotti et al. 1998). The other part of the algorithm uses a nonlinear regression analysis through the Levenberg-Marquardt subroutine to minimize the fitting error on the average, thus providing an improved final set $\{\lambda_m, g_m\}$. The following steps are carried out in this sense:

***Step 1***. We form a grid for relaxation times, $\lambda_1 < \lambda_2 < ... < \lambda_M$, where $\lambda_i = \lambda_{\min}\left(\frac{\lambda_{\max}}{\lambda_{\min}}\right)^{\frac{i-1}{M-1}}$ with $i$=1…$M$. Since experimental data are obtained for the frequency range $\omega_{min}<\omega<\omega_{max}$, $\lambda_{\min}=1/\omega_{\max}$ and $\lambda_{\max}=1/\omega_{\min}$ are defined. It is suggested to use $M \cong 30$ (see also Honerkamp and Weese, 1989).

***Step 2***. Minimizing $\left\|\underline{\underline{K}}\cdot\underline{h}-\underline{G}\right\|$ is required with the unknown $\underline{h}=\{g_m\}$ for $m$=1…$M$, subject to, $\underline{h}>0$, where $\underline{\underline{K}}$ is a $2N$ x $M$ matrix, $\underline{G}$ is a $2N$ vector, and $\underline{h}$ is an $M$ vector. Additionally, $N$ is the number of frequency values in order to obtain experimental data of the storage and dissipation modules, which are designated here $G_i'(\omega_i)$ and $G_i''(\omega_i)$, respectively, for $i$=1…$N$. The number of discrete relaxation times is $M$, and the algorithm requires that $N \geq M$. Therefore, from the linear viscoelasticity (Eqs. (4) and (5)), we define, $K_{i,m}=\frac{\lambda_m^2\omega_i^2}{1+\lambda_m^2\omega_i^2}$, for $i$=1…$N$, and $m$=1…$M$, and $K_{i,m}=\frac{\lambda_m\omega_i}{1+\lambda_m^2\omega_i^2}$, for $i$=$N$+1…2$N$, and $m$=1…$M$. The components $G_i$ of vector $\underline{G}$ have to be assigned as follows: $G_i=G_i'(\omega_i)$, for $i$=1…$N$, and $G_i=G_i''(\omega_i)$, for $i$=$N$+1…2$N$.

***Step 3***. We apply the algorithm presented by Lawson and Hanson (1974). It should be observed that in this numerical code there are two vectors $\underline{P}$ and $\underline{Z}$, the dimensions of which are $P$ and $Z$ respectively. These dimensions change along the iterative process so that $P$+$Z$=$N$.

Therefore, once the convergence is attained, one gets, $g_m > 0$, for $m$=1…$P$ and $g_m = 0$ for $m$=$P$+1…$M$. Of course, the vector $\underline{h} = \{g_m\}$ with $g_m > 0$ and dimension $P$<$N$, satisfies, $\frac{\left|\underline{\underline{K}} \cdot \underline{h} - \underline{G}\right|}{\left|\underline{G}\right|} = E_1$, where $E_1 \leq 1\%$ typically for the polyethylene samples. Thus, at this step, we get the spectrum $\{\lambda_m, g_m\}$, where $\lambda_m$ for $m$=1… $P$ are the remaining values of the original set.

***Step 4***. One can still try to improve the fitting of experimental data $G_i'(\omega_i)$ and $G_i''(\omega_i)$ by using the well-known Levenberg-Marquardt routine. Therefore, this code is initialized with $\{\lambda_m, g_m\}$ obtained at Step 3. In this routine, we define $2N$ nonlinear algebraic equations $f_1 \ldots f_{2N}$ for the unknown vector $\underline{x} = \{\lambda_1 \ldots \lambda_p, g_1 \ldots g_p\}$, where $f_i = K'_{i,m} - G_i$. Thus one gets, $K'_{i,m} = \sum_{m=1}^{M} g_m \frac{\omega_i^2 \lambda_m^2}{1+\omega_i^2 \lambda_m^2}$, for $i$=1…$N$, and $m$=1…$P$, and $K'_{i,m} = \sum_{m=1}^{M} g_m \frac{\omega_i \lambda_m}{1+\omega_i^2 \lambda_m^2}$, for $i$=$N$+1…2$N$ and $m$=1…$P$. $G_i$ are the same as those components defined above. Therefore, the target is the minimization of $\left\|\underline{f}\right\|^2$ where the component of vector $\underline{f} = \{f_i\}$ is also defined above. Once the convergence is attained, this code gives us a new spectrum $\{\lambda_m, g_m\}$ of dimension $P$ as in Step 3. The convergence error is designated $E_2$ and it is defined with an expression similar to $E_1$. In general $E_2 \leq E_1$ but this cannot always be assured.

Once the spectrum of relaxation times is available, the shear modulus $G(t)$ may be obtained having into account that the asymptotic behavior describing the linear viscoelastic response relates directly $G'$ and $G''$ to $G(t)$ through Fourier transform. Thus, the transform variables are frequency $\omega$ and time $t$, and the relevant expression obtained is,

$$G(t) = \sum_{m=1}^{M} g_m \exp(-t/\lambda_m) \tag{6}$$

The next step is therefore to calculate important linear viscoelastic parameters of the polymer melts like: plateau modulus $G_N^o$, zero shear rate viscosity $\eta_o$, rubbery plateau relaxation time $\lambda_N^o$ and steady state compliance $J_e^o$, which may be obtained from the following equations of the linear viscoelastic theory, involving the set $\{\lambda_m, g_m\}$ obtained with Eqs. (4) and (5):

$$G_N^o = \frac{2}{\pi} \int_o^\infty \frac{G''(\omega)}{\omega} d\omega = \sum_{m=1}^{M} g_m \tag{7}$$

$$\eta_o = \int_o^\infty G(t) dt = \sum_{m=1}^{M} g_m \lambda_m \tag{8}$$

$$\lambda_N^o = \frac{\eta_o}{G_N^o} \tag{9}$$

$$J_e^o = \frac{\sum_{m=1}^{M} g_m \lambda_m^2}{\eta_o{}^2} \tag{10}$$

## 3 RHEOMETRIC CHARACTERIZATION OF MELTS IN THE NONLINEAR VISCOELASTIC RESPONSE FOR SHEAR FLOW

When a constant shear rate flow is suddenly imposed to a polymer melt, the rate of strain tensor is expressed,

$$\underline{\underline{D}} = \begin{Bmatrix} 0 & \frac{1}{2}\dot{\gamma} & 0 \\ \frac{1}{2}\dot{\gamma} & 0 & 0 \\ 0 & 0 & 0 \end{Bmatrix} \tag{11}$$

where $\dot{\gamma}$ is the constant shear rate. Therefore, combining Eqs. (1) to (3) with Eq. (11) the components of the stress tensor may be evaluated from the following evolution equations, expressed through cylindrical coordinates for practical reasons:

$$\frac{\partial \tau_m^{zz}}{\partial t} = -\frac{K_m}{\lambda_m}\tau_m^{zz} + \tau_m^{rz}\dot{\gamma}\left(1-\frac{\chi}{2}\right) + \tau_m^{zr}\dot{\gamma}\left(1-\frac{\chi}{2}\right) \tag{12}$$

$$\frac{\partial \tau_m^{rr}}{\partial t} = -\frac{K_m}{\lambda_m}\tau_m^{rr} - \tau_m^{rz}\dot{\gamma}\frac{\chi}{2} - \tau_m^{zr}\dot{\gamma}\frac{\chi}{2} \tag{13}$$

$$\frac{\partial \tau_m^{zr}}{\partial t} = -\frac{K_m}{\lambda_m}\tau_m^{zr} + \tau_m^{rr}\dot{\gamma}\left(1-\frac{\chi}{2}\right) - \tau_m^{zz}\dot{\gamma}\frac{\chi}{2} + g_m\dot{\gamma} \tag{14}$$

$$\frac{\partial \tau_m^{\theta\theta}}{\partial t} = -\frac{K_m}{\lambda_m}\tau_m^{\theta\theta} \tag{15}$$

$$K_m = exp\left[\frac{\xi}{g_m}\left(\tau_m^{zz} + \tau_m^{rr} + \tau_m^{\theta\theta}\right)\right]. \tag{16}$$

for $m = 1...M$ , where $\dot{\gamma} = dv_z / dr$ . In addition, $\tau_s^{zz} = \tau_s^{rr} = \tau_s^{\theta\theta} = 0$ and $\tau_s^{zr} = \eta_s\dot{\gamma}$ .

A procedure to find the shear stress $\tau = \tau^{zr} = \sum_{m=1}^{M}\tau_m^{zr} + \tau_s^{zr}$ and the shear rate viscosity $\eta = \tau/\dot{\gamma}$ is to solve these equations numerically from the inception of the shear flow until the asymptotic steady state is reached. In order to calculate this steady state, the time derivatives in Eqs. (12) to (15) are written in discrete form (forward finite differences). Then the fourth order Runge-Kutta method is applied until stresses are constant. The time step used in this work is $10^{-5}$ s. Criteria for convergence to the steady state are expressed in terms of two consecutive time steps, as follows,

$$\frac{\left|\left(\sum_{m=1}^{M}\tau_m^{pq}\right)^{i+1}-\left(\sum_{m=1}^{M}\tau_m^{pq}\right)^{i}\right|}{\left|\left(\sum_{m=1}^{M}\tau_m^{pq}\right)^{i}\right|}\leq 10^{-6} \tag{17}$$

where superscripts *p* and *q* refer to cylindrical coordinates (see Eqs. (12) to (16)) and *i* indicates the number of time steps being carried out.

## 4 RHEOMETRIC CHARACTERIZATION OF MELTS IN THE NONLINEAR VISCOELASTIC RESPONSE FOR ELONGATIONAL FLOW

For the purpose of visualizing the behavior of the polyethylene melt samples under rheometric elongational flow, a constant elongational rate $\dot{\varepsilon}$ is suddenly imposed to the PTT model representing the polymer melt samples. Therefore, the rate of strain tensor is expressed,

$$\underline{\underline{D}}=\begin{Bmatrix}\dot{\varepsilon} & 0 & 0\\ 0 & -\frac{1}{2}\dot{\varepsilon} & 0\\ 0 & 0 & -\frac{1}{2}\dot{\varepsilon}\end{Bmatrix} \tag{18}$$

In this case, $\tau_m^{rr}=\tau_m^{\theta\theta}$ is satisfied. For the elongational flow, stresses at the steady state regime cannot be obtained explicitly with the spectral PTT model. Therefore, the elongational viscosity $\eta_e=\left(\sum_{m=1}^{M}\tau_m^{zz}-\sum_{m=1}^{M}\tau_m^{rr}\right)/\dot{\varepsilon}$ is found here by solving numerically the following evolution equations, for the inception of the elongational flow, until the asymptotic steady state is reached,

$$\frac{\partial\tau_m^{zz}}{\partial t}=-\frac{K_m}{\lambda_m}\tau_m^{zz}+2\tau_m^{zz}(1-\chi)\dot{\varepsilon}+2g_m\dot{\varepsilon} \tag{19}$$

$$\frac{\partial\tau_m^{rr}}{\partial t}=-\frac{K_m}{\lambda_m}\tau_m^{rr}-\tau_m^{rr}(1-\chi)\dot{\varepsilon}-g_m\dot{\varepsilon} \tag{20}$$

$$\frac{\partial\tau_m^{\theta\theta}}{\partial t}=-\frac{K_m}{\lambda_m}\tau_m^{\theta\theta}-\tau_m^{\theta\theta}(1-\chi)\dot{\varepsilon}-g_m\dot{\varepsilon} \tag{21}$$

$$K_m=exp\left[\frac{\xi}{g_m}\left(\tau_m^{zz}+2\tau_m^{rr}\right)\right]. \tag{22}$$

where, $m=1...M$ .

Once more, in order to find the steady state stresses, time derivatives in Eqs. (19) to (21) are written in discrete form. Then the same numerical procedure as that used for the shear flow analyzed above is applied.

## 4 RESULTS AND DISCUSSION

In this section, first the numerical results obtained for the set $\{\lambda_m, g_m\}$ within the framework of linear viscoelasticity are discussed briefly. Then stress evolutions described by Eqs. (11) to (16) and (18) to (22) involving finite constant shear rate and constant elongational rate, respectively, are solved numerically and discussed in relation to experimental data available in the literature. These results are presented and discussed in the same order as they have been formulated above. Finally transient responses of shear and elongational rheometric functions are illustrated and analyzed for the three polyethylene melt samples under study.

### 4.1 Linear viscoelasticity

Figure 1 (a, b and c) shows the storage and loss modules $G'$ and $G''$ as functions of frequency $\omega$, for the three polyethylene samples in the melt state. One observes in this figure that the fittings (solid lines) of experimental data (symbols) are accomplished well with the spectrum of relaxation times calculated here, which in general do not exceed eight modes. We have also plotted the modulus of the complex dynamic viscosity to show the pseudoplastic responses of the three polymer melts (see also the experimental shear viscosity functions below), which may be inferred consistently through the well known and approximate Cox-Merz rule.

It is also relevant to point out here that the HDPE1 sample shows the lower crossover frequency, as it is observed in Figure 1 (a, b and c), indicating that this melt has values of relaxation times higher than those pertaining to LLDPE1 and LDPE9 samples. This result is consistent with the characteristic values reported in Table 1 (see also Table 2). Thus, HDPE1 has the higher average molecular weight apart from being morphologically linear.

Figure 2 shows the relaxation modulus $G(t)$ for the three polyethylene melt samples. It is found that the magnitude of the rubbery transition is quite significant for LLDPE1, what is consistent with the high value of $G_N^o$ found for this polymer (see Table 2 and Eqs. (7) to (10)). Thus the morphologies of HDPE1 and LLDPE1 samples, apart from both being linear polymers, present in addition other different characteristics: thus, average molecular weights affect directly the value of $\eta_o$, but this is not necessarily true for the interpretation of $G_N^o$ as expected from the theory of rubber elasticity. In fact $G_N^o \propto nk_BT$, where $n$ is the number of entanglement per unit volume, $k_B$ is the Boltzman constant and $T$ the absolute temperature. Consequently, one should not expect to find an important incidence of the average molecular weight on $G_N^o$. On the other hand, polydispersity is relevant in the determination of $G_N^o$, and this effect can be visualized from the theory of rubber elasticity when one corrects the shear modulus expression by the presence of unentangled chain terminals in the network. This effect is clearly illustrated in Table 2 through HDPE1 and LLDPE1 samples.

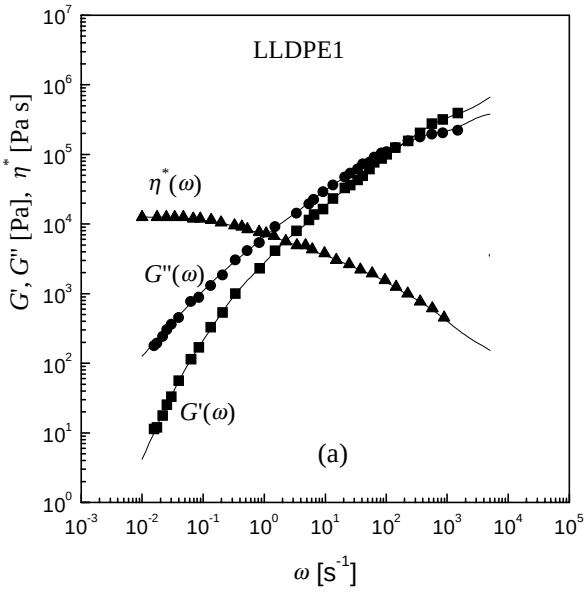


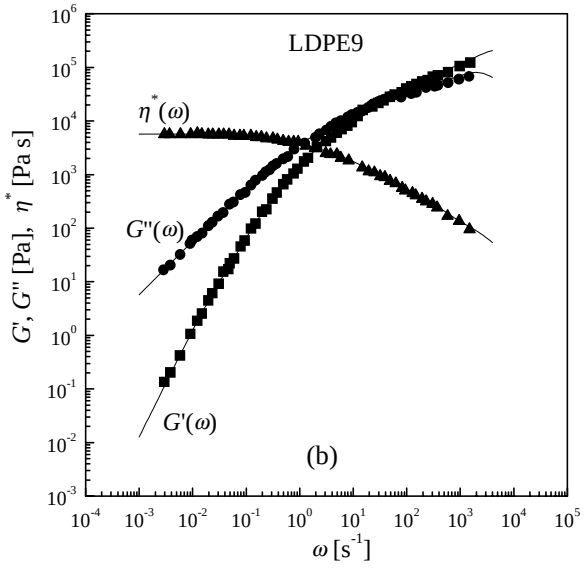

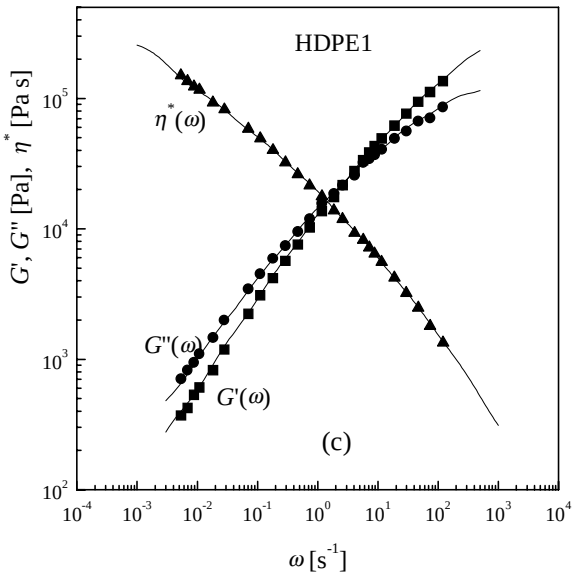


Figure 1**:** Storage and loss modules $G'$ and $G''$ and complex dynamic viscosity modulus $\eta^*$ for melts LLDPE1, LDPE9, and HDPE1 at 190 $^o$C. Experimental data (symbols) are obtained from Bennart (2001). Solid lines show the fittings of these experimental data with Eqs. (4) and (5) determining the relaxation time spectrum.

Table 2 also shows that numerical predictions of $\eta_o$ compare well with those values obtained by Bernnat (2001), indicating a good convergence of the numerical algorithm generated here to fit experimental data with Eqs. (4) and (5). It is also evident that $J_N^o$ behaves inversely proportional to $G_N^o$ as one should expect from the theory of linear viscoelasticity, while the characteristic relaxation time $\lambda_N^o$ is the result of a rather complex coupling between different effects manifested through $G_N^o$ and $\eta_o$. In fact, reptation of chains in a polydisperse melt, giving the relation $\eta_o \propto M_w^\alpha$ with approximately $\alpha \approx 3.4$ (samples tested here are not strictly monodiperse chains), also involves the tube release mechanism, which is associated with local Rouse type relaxation modes of the entangled network (Deiber et al., 2002; Peirotti and Deiber, 2003), affected in part by the polymer density. As one expects, the branched LDPE9 sample gives the lower $G_N^o$, which should not be affected ideally by the average molecular weight.

| Sample | $G_N^o$ [Pa] | $\lambda_N^o$ [s] | $J_e^o$ [Pa$^{-1}$] | $\eta_o$ [Pa s] | $\eta_o$ [Pa s] (Bernnat, 2001) |
|---|---|---|---|---|---|
| LLDPE1 | $1.08\ 10^6$ | $1.17\ 10^{-2}$ | $2.66\ 10^{-4}$ | $1.26\ 10^4$ | $1.265\ 10^4$ |
| LDPE9 | $2.10\ 10^5$ | $2.73\ 10^{-2}$ | $3.88\ 10^{-4}$ | $5.74\ 10^3$ | $5.74\ 10^3$ |
| HDPE1 | $6.23\ 10^5$ | $4.46\ 10^{-1}$ | $1.09\ 10^{-3}$ | $2.78\ 10^5$ | $2.75\ 10^5$ |

Table 2**:** Material properties calculated from Eqs. (7) to (10) for the three polyethylene melt samples.

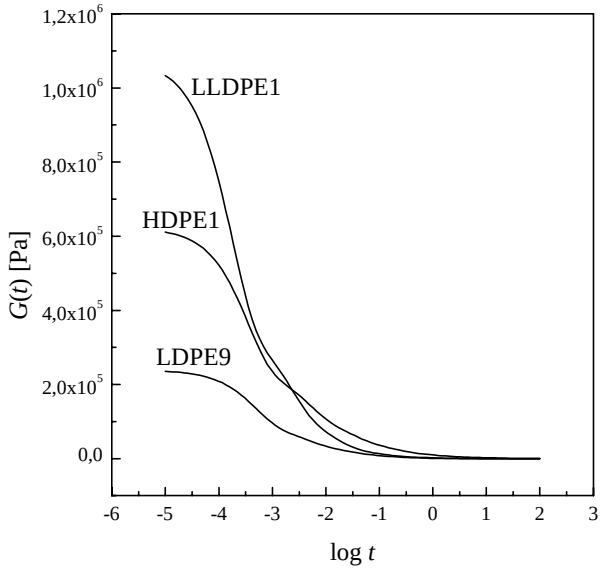


Figure 2: Shear relaxation modulus $G(t)$ from Eq. (6) for LLDPE1, LDPE9 and HDPE1.

## 4.2 Shear and elongational flows

Figure 3 shows the fitting of experimental data of both shear and elongational viscosities through the PTT model (Eqs. (1) to (3)) and the numerical code proposed and explained above in relation to Eqs. (11) to (22). Through these calculations, the fitting parameters found numerically are $\chi = 0.1$, $\alpha \to 1$ and those reported in Table 3 for $\xi$.

| Polyethylene | $\xi$ |
|---|---|
| LDPE9 | 0.013 |
| LLDPE1 | 0.08 |
| HDPE1 | 0.1 |

Table 3: Values of parameter $\xi$ for polyethylene melt samples.

Thus, it is clear that $\chi$ and $\alpha$ are not sensitive to chain structure of the polyethylene melts studied here, while $\xi$ increases with the average molecular weight (see also Table 1). Also this parameter is higher for melts with linear chains.

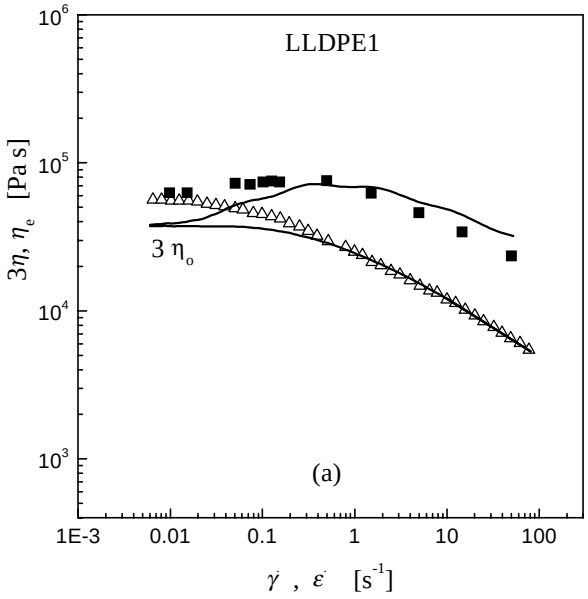


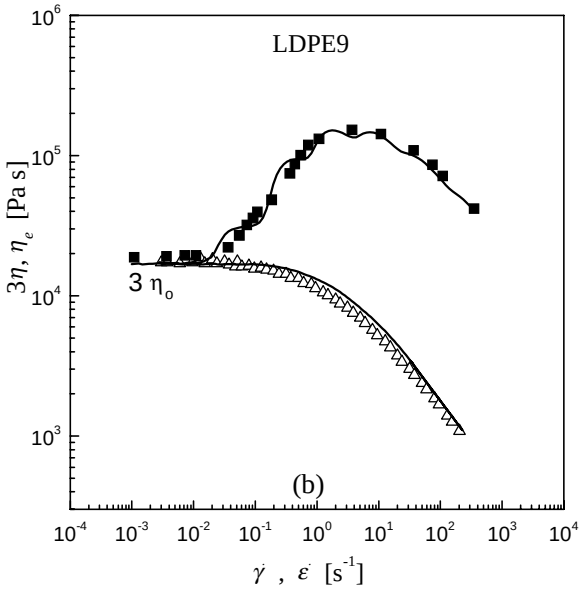

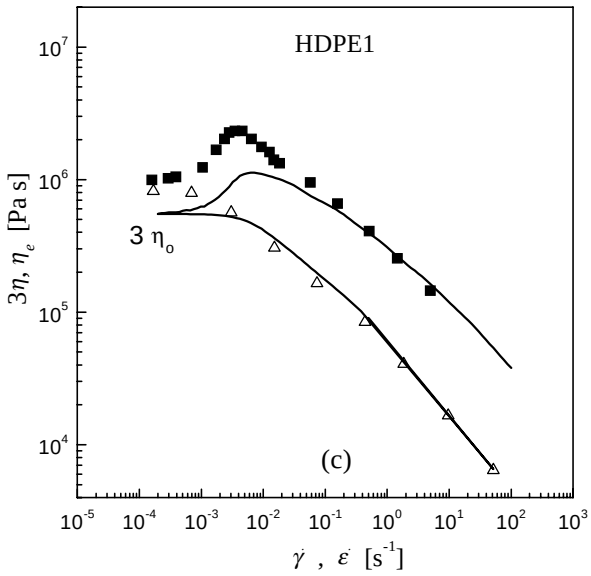


Figure 3: Steady state shear and elongational viscosities calculated with the spectral PTT model (solid lines). Symbols are experimental data reported by Bernnat (2001).

From Figure 3 one concludes that the branched polymer melt of the same chemical type as linear ones present a higher resistance to elongation, which is visualized as the difference between the Trouton viscosity asymptote and the maximum peak of the elongational viscosity. Also, having into account that Figure 3 reports nonlinear rheometric functions and includes experimental data of elongational and shear rheometries, one may conclude that the PTT model is appropriate to represent rheologically linear and branched polyethylene melts, despite some differences may be visualized between numerical predictions and experimental data in the case of the linear polymer melts. What is more relevant here is the consistency found in predicting stresses well, for two independent mechanical histories like the imposition of constant shear and elongational rates. These types of predictions with experimental validations involving both shear and elongational rates have been rarely found in the literature. Analyzing even more deeply Figure 3, it is evident that the PTT model is much better for the branched polyethylene melt. Nevertheless, in relation to this result one should also consider that the measurement of the elongational viscosity has been quite difficult to obtain with the present state of the art of rheometry, and hence some experimental shifting errors could be also associated with the results reported in Figure 3, although they were present only for the linear polymer melts. Thus systematic shifts in the Trouton asymptotes for the two linear polyethylene melts are visualized in Figure 3 (a and c), in contraposition to Figure 3 (b), where this asymptote is satisfied remarkably well.

### 4.3 Simulation of transient shear and elongational flows

Once both linear and some relevant steady nonlinear viscoelastic responses of the spectral PTT model have been fitted to the corresponding rheometric experimental data, allowing one to determine rheological parameters $\{\lambda_m, g_m\}$, $\alpha$, $\chi$ and $\xi$, it is now possible to simulate the transient response of the three polyethylene melt samples to obtain further rheological conclusions.

Figure 4 (a, b and c), for instance, illustrates the transient shear viscosity upon inception of a constant shear rate $\dot{\gamma}_o$. Although one may observe that overshooting of the shear viscosity function increases with the intensity of shear rate, which is a well known result for polymer melts in general, it is also possible to visualize that overshooting magnitudes are higher for increasing molecular weight mainly for linear chain melts. In addition, one finds that the dumping of the viscosity function at high values of time may present oscillations of high frequency for HDPE1 and LLDPE1 (the linear samples) in contraposition to the branched LDPE9 sample, which for a shear rate of 0.1 $s^{-1}$ does not show neither overshoot nor oscillations. These results are in part a consequence of the type of convected derivative used in the PTT model involving the magnitude of parameter $\chi$. In fact as $\chi$ increases, the Gordon-Schowalter derivative becomes more corrotational than codeformational. Therefore, as it is well known, the oscillations at high times for $\chi \neq 0$ are expected.

Figure 5 (a, b and c), for instance, illustrates the transient elongational viscosity upon inception of a constant elongational rate $\dot{\varepsilon}_o$. One may observe here how the transient growing elongational viscosity increases toward the asymptotic steady state value. These figures reproduce also the experimental responses typically found with polymer melts under the transient elongational test, by showing how difficult may result to attain the asymptotic steady state value of the elongational viscosity.

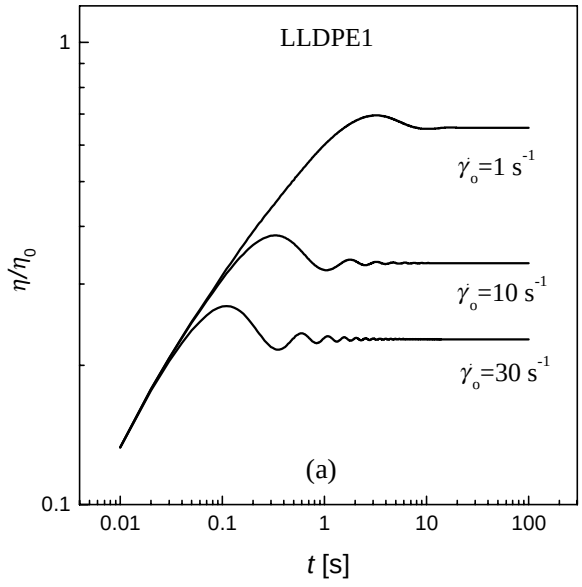

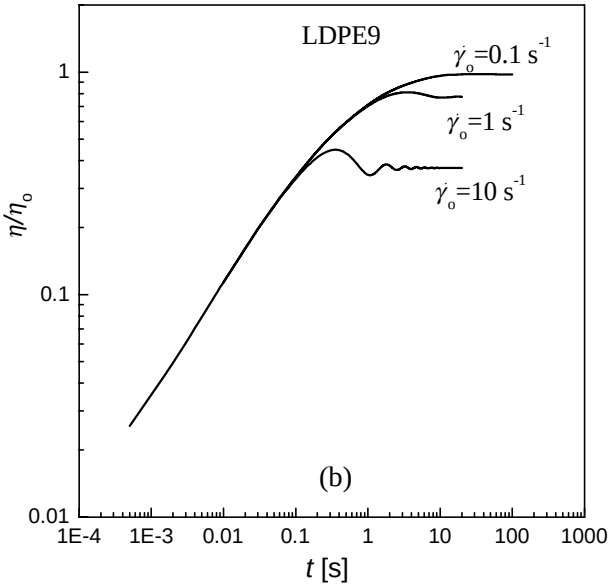


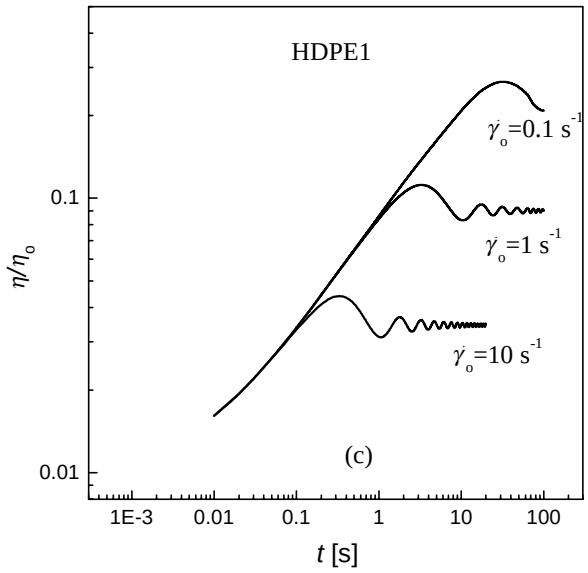


Figure 4: Transient shear viscosity of melts for different constant shear rate $\dot{\gamma}_o$ :
(a) LLDPE1, (b) LDPE9, (c) HDPE1.

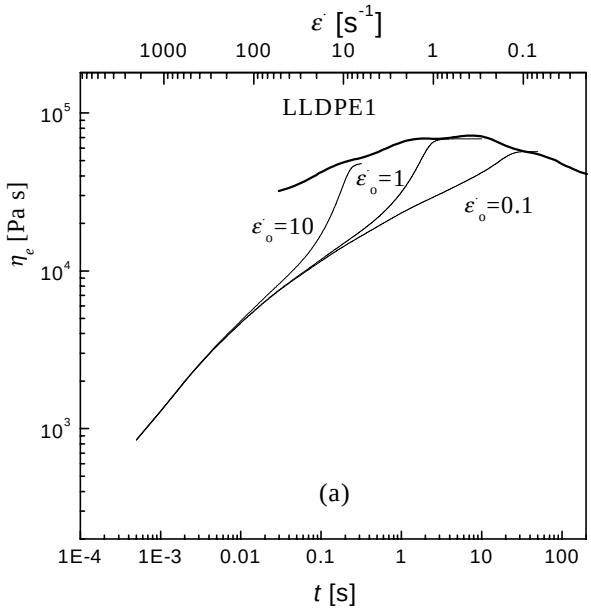


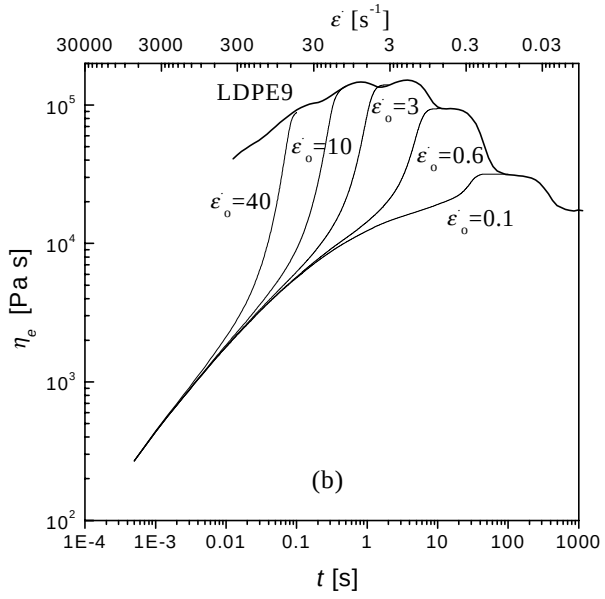

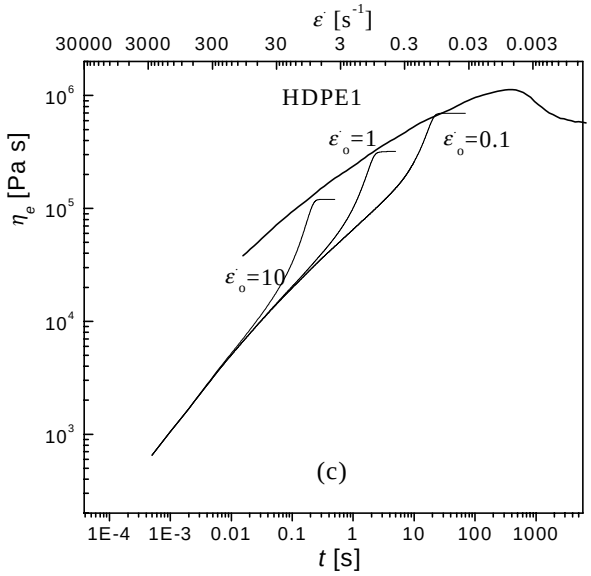


Figure 5**:** Transient elongational viscosity of melts for different constant elongational $\dot{\varepsilon}_o$: (a) LLDPE1, (b) LDPE9, (c) HDPE1.

## 5 CONCLUSIONS

One of the relevant conclusions obtained here is that an appropriate selection of constitutive equations for the stress tensor of polymer melts, like linear and branched polyethylene melts, may be carried out only when experimental data of rheometric functions pertaining to both the linear and nonlinear viscoelastic responses are available, involving both shear and elongational kinematics. Under these circumstances the full set of rheological parameters pertaining to a constitutive equation may be evaluated consistently and without ambiguity (gross hypothesis and approximations may be thus avoided). In this sense it is clear that researches on elongational rheometry is a subject of relevance in rheology to be one able to characterize materials in the processing industry. More specifically, we found that the PTT model is excellent for the branched LDPE9 polyethylene melt. Thus one expects that the rheological characterization of this melt through the spectral PTT model may be used with sufficient precision in the prediction of complex flows found in processing operations. More generally, the selection of a constitutive equation for a given material requires a relevant set of experimental data concerning different rheometric tests and, what is not less important, the availability of robust algorithms, which are able to solve any steady and transient mechanical histories. These algorithms must also fit experimental data and simulate any steady and transient material responses.

## REFERENCES

A. Bernnat. Polymer Melt Rheology and the Rheotens Test. Doctoral Thesis, 2001.

J.A. Deiber, M.B. Peirotti and A. Gappa. The linear viscoelastic relaxation modulus related to the MWD of linear homopolymer blends. *J. of Elastomers and Plastics*, 29:290–313, 1997.

J.A.Deiber, M.B. Peirotti, M.A. Villar, J.A. Ressia and E.M. Vallés. Linear viscoelastic relaxation modulus of polydisperse poly(dimethylsiloxane) melts containing unentangled chains. *Polymer*, 43:3035–304, 2002.

R.J. Gordon and W.R. Schowalter. Anisotropic Fluid Theory: a Different Approached to the Dumbbell Theory of Dilute Polymer Solutions, *Trans. Soc. Rheol.*, 16:79-97, 1972.

J. Honerkamp and J. Weese. Determination of the relaxation spectrum by a regularization method. *Macromolecules*, 22: 4372 – 4377, 1989.

C.L. Lawson and R.H. Hanson. *Solving least squares problems*. New Jersey: Prentice Hall, Inc., 1974.

M.B. Peirotti and J.A. Deiber. Estimation of the molecular weight distribution of linear homopolymer blends from linear viscoelasticity for bimodal and high polydisperse samples. *Lat. Am. Appl. Res.*, 33:185-194, 2003.

M.B. Peirotti, J.A. Deiber, J.A. Ressia, M.A. Villar and E.M. Vallés. Relaxation modes of molten polydimethylsiloxane. *Rheologica Acta*, 37:449–462, 1998.